

# PHYSICAL REVIEW LETTERS

VOLUME 31

29 OCTOBER 1973

NUMBER 18

## Glauber-Theory Approach for Molecular Vibrational Excitations\*

T. N. Chang, Robert T. Poe, and Pritam Ray

*Department of Physics, University of California, Riverside, California 92507*

(Received 13 August 1973)

Molecular vibrational excitations by charged-particle impact are investigated within the Glauber-theory approach. Theoretical results for electron- $H_2$  scattering give good agreement with experimental data. We study the physical effects responsible for the structures in the differential cross section.

Recent experiments<sup>1</sup> on the vibrational-rotational excitations of molecules by charged-particle impact at intermediate and high energies have revealed considerable distinct features. The multicentered nature of the target molecule, along with the complexity of possible excitation channels, effectively precludes a first-principles theoretical treatment; one is therefore led to seek to understand the excitation process through approaches with simplified assumptions. In this note we report the result of such a study. Two dominant physical processes for the vibrational excitations of molecules are taken into account. Calculations are carried out within the framework of the Glauber theory.<sup>2</sup> Results of our calculation for  $e-H_2$  vibrational excitation show good agreement with experimental data. In addition, much qualitative understanding of the excitation mechanism can be gained.

Physical considerations of the vibrational excitation process suggest that two leading mechanisms take place in two distinct physical regions.<sup>3</sup>

(1) Large-impact-parameter region. Here the incident charged particle "sees" the target molecule as a whole, and excitations are induced through the long-range dipole polarization potential. The Buckingham-type potential  $V_p = -\alpha/2(r^2 + a_p^2)^2$  is often used in atomic scattering problems; but for molecular problems an additional

factor  $1 - \exp[-(r/a_p)^5]$  is needed<sup>4</sup> to account for the larger excitation channels or absorption effects. The average molecular dipole polarizability  $\alpha(R)$  is a function of the interatomic separation  $R$ . For our  $H_2$  calculation, we use tabulated values of  $\alpha(R)$  by Kolos and Wolniewicz.<sup>5</sup>

(2) Small-impact-parameter region. Here the incident particle comes closely and will "see" each individual atomic center of the target molecule. The important point here is to recognize that molecular vibrational and rotational excitations must proceed mainly through energy-momentum transfer imparted directly to the heavy atomic nuclei. That is, excitations come mostly from the direct encounter between the incident particle and the atomic nuclei of the target, with the molecular electron clouds  $p$  playing mainly the role of shielding. The effective potential for each atomic center is thus

$$V(r) = -Z/r + \int d^3r' \rho(r')/|\vec{r} - \vec{r}'|. \quad (1)$$

For the  $H_2$  case, this is well approximated by

$$V(r) = (1/r + Z)e^{-Zr}, \quad (2)$$

with  $Z = 1.166$ .<sup>6</sup> Other interactions such as exchange and quadrupole will have only a secondary effect for the energy range considered.

We proceed to calculate the differential cross sections for vibrational excitations within the framework of the Glauber-theory approach.<sup>2</sup> The

Glauber formulation, developed originally in the context of nuclear physics, has recently been applied to electron-atom scatterings with considerable success.<sup>7</sup> Here we mention two features particularly salient for molecular scattering calculations. First, difficult calculations of a multicentered nature never appear directly in the present formulation, and it is one of the aims of this paper to show that good results can be obtained without such calculations. Secondly, the approach easily lends itself to multiple-scattering decompositions, hence the study of single and double scattering.

With the Glauber formalism, the relevant equations are

$$\left(\frac{d\sigma}{d\Omega}\right)_{fi} = \frac{k_f}{k_i} |\langle f | G(\vec{q}, \vec{s}) | i \rangle|^2, \quad (3)$$

$$G(\vec{q}, \vec{s}) = \frac{ik_i}{2\pi} \int d^2b e^{i\vec{q}\cdot\vec{b}} [1 - e^{i\chi(\vec{b}, \vec{s})}], \quad (4)$$

where

$$\chi(\vec{b}, \vec{s}) = -k_i^{-1} \int_{-\infty}^{+\infty} V(\vec{b} + \hat{k}z, \vec{R}) dz \quad (5)$$

is the Glauber phase-shift function,  $\vec{b}$  the impact parameter,  $\vec{R} = \vec{s} + \hat{k}z$  the interatomic vector, and  $\vec{q} = \vec{k}_i - \vec{k}_f$  the momentum transfer in the excitation process. The path of integration  $z$  is along the incident direction, the center of coordinates

being the middle of the nuclei. All rotational wave-function states are explicitly summed up to provide direct comparison with experiment. For the vibrational wave functions, the Morse function<sup>8</sup> has been used. While the expressions contain up to five in total dimensionality, the symmetry properties contained therein still keep the computational effort on a quite modest level.

The angular distributions for  $\nu=0$  to  $\nu=1$  excitations in the energy range 20 to 81.6 eV, along with the corresponding experimental data, are given in Fig. 1. It is seen that theoretical result is able to yield the observed structures as well as a good overall quantitative agreement, even at an energy as low as 20 eV. As the energy increases, our theoretical results predict that the dip structure becomes more pronounced and moves toward small angles, again in agreement with the experimental indications. The breakdown of contributions from different physical effects as given by the Glauber-theory result is illustrated in Fig. 2. It is seen that the sharp forward peak comes from the long-range polarization effect. The broad secondary maximum at large angles comes from short-range collisions with individual atomic nuclei. At even higher energies (not illustrated), we find that the forward peak narrows steadily and small-impact-parameter collisions become dominant at all angles. The double-scattering contribution, in this energy range, is shadowed by the polarization contribution at small angles and by single-scattering

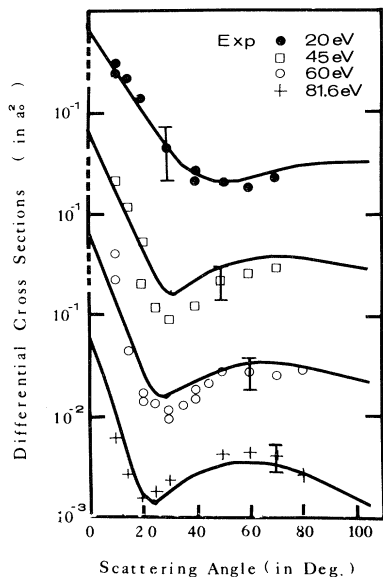


FIG. 1. Differential cross sections for the 0-1 vibrational excitation of  $H_2$  by 20-, 45-, 60-, and 81.6-eV electrons. Solid lines, results of the present calculation. The corresponding experimental results are taken from Ref. 1.

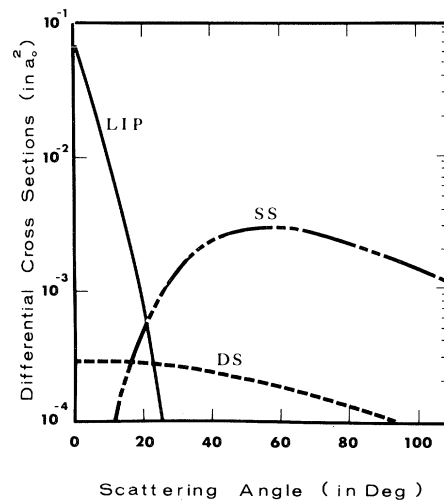


FIG. 2. Contributions from various physical effects (large impact parameter, single scattering, double scattering) to the differential cross sections for the 0-1 vibrational excitation of  $H_2$  by 81.6-eV electrons.

tering contributions at large angles. However, from our calculations the double scattering will become more important for higher vibrational-level excitations or at lower electron impact energies. These and other results will be reported later in a detailed publication. The excellent result from the present calculation encourages further exploration of this simplified general approach for the molecular vibrational excitations.

It is a pleasure to acknowledge valuable discussions with Dr. S. Trajmar and Dr. D. G. Truhlar.

\*Research supported in part by the National Aeronautics and Space Administration.

<sup>1</sup>S. Trajmar, D. G. Truhlar, J. K. Rice, and A. Kupfermann, *J. Chem. Phys.* **52**, 4516 (1970).

<sup>2</sup>R. J. Glauber, in *Lectures in Theoretical Physics*,

edited by W. E. Brittin *et al.*, (Interscience, New York, 1959), Vol. I, p. 315; V. Franco and R. J. Glauber, *Phys. Rev.* **142**, 1195 (1966).

<sup>3</sup>This separation of the two regions is only meant for a physical description. In actual calculation, no critical impact parameter is needed to divide the two regions. Rather, the cross-section contributions from these two potentials are simply calculated separately and then summed.

<sup>4</sup>D. G. Truhlar and J. K. Rice, *J. Chem. Phys.* **52**, 4480 (1970), and references therein. We have used the value of  $1.8a_0$  for the cutoff parameter  $a_p$ , consistent with those obtained by others.

<sup>5</sup>W. Kolos and L. Wolniewicz, *J. Chem. Phys.* **46**, 1426 (1967).

<sup>6</sup>S. C. Wang, *Phys. Rev.* **31**, 579 (1928).

<sup>7</sup>V. Franco, *Phys. Rev. Lett.* **20**, 709 (1968); H. Tai, R. H. Bassel, E. Gerjuoy, and V. Franco, *Phys. Rev. A* **1**, 1819 (1970); F. W. Byron, Jr., *Phys. Rev. A* **4**, 1907 (1971).

<sup>8</sup>P. M. Morse, *Phys. Rev.* **34**, 57 (1929).

## Radiative Capture and Bremsstrahlung of Bound Electrons Induced by Heavy Ions\*

P. Kienle,† M. Kleber,† B. Povh,‡ R. M. Diamond, F. S. Stephens,  
E. Grosse,§ M. R. Maier,† and D. Proetel†

*Lawrence Berkeley Laboratory, University of California, Berkeley, California 94720*

(Received 31 July 1973)

X rays emitted during the radiative capture of target electrons into the *K* shell of fast and highly stripped projectiles were observed. When using targets with strongly bound electrons, a high-energy x-ray tail was also found; this new process is a type of electron bremsstrahlung. The cross sections for both these processes can be explained quantitatively.

In the x-ray emission accompanying the passage of fast highly stripped heavy ions through gases, we have been able to distinguish three types of beam-associated radiation:

(1) Characteristic x rays emitted following electron transfer into the *L*, *M*, and outer shells of a stripped ion.

(2) A broad x-ray band from the radiative capture of bound electrons from the target into the *K* shell of the fast projectile. The energies correspond to the difference of the electron binding energies in the initial and final state plus the electron kinetic energy relative to the projectile, and reflect the momentum distribution of the bound electrons. This radiation has been recently identified by Schnopper *et al.*<sup>1</sup>

(3) A high-energy tail going up to an energy corresponding roughly to  $\hbar v/a$ , where  $v$  is the projectile velocity and  $a$  is equal to the Bohr radius. This new process we ascribe to brems-

strahlung from initially bound target electrons in the Coulomb field of the projectile.

The x-ray emission was studied when high-energy <sup>40</sup>Ar, <sup>20</sup>Ne, and <sup>14</sup>N beams passed through targets of gaseous molecules and simple noble gases up to argon. Beams of <sup>40</sup>Ar were obtained from the Lawrence Berkeley Laboratory (LBL) SuperHILAC (heavy-ion linear accelerator) at energies up to 288 MeV (7.2 MeV/nucleon) and then stripped in the 6- $\mu$ m Al entrance window of the gas target cell to an equilibrium average state of about 17<sup>+</sup>. The <sup>20</sup>Ne and <sup>14</sup>N were accelerated in the LBL 88-in. cyclotron to 140 MeV (7.0 MeV/nucleon) and to 160 MeV (11.4 MeV/nucleon) and 250 MeV (17.9 MeV/nucleon), respectively, and were essentially completely stripped upon entering the gas target. The x-ray spectrometer was a 5-mm-diam Si detector coupled to a low-noise pulsed-light feedback amplifier with a peaking time of 9.5  $\mu$ sec and a fast pileup rejector. The